Acta Cryst. (1996). A52, 413–418

Theoretical Structure Factors and Electron Density of Magnesite ($MgCO_3$)

M. CATTI[a] AND A. PAVESE[b]*

[a]*Dipartimento di Chimica Fisica ed Elettrochimica, Università degli Studi di Milano, Via Golgi 19, Milano 20133, Italy, and* [b]*Dipartimento Scienze della Terra, Sezione Mineralogia, Università degli Studi di Milano, Via Botticelli 23, Milano 20133, Italy. E-mail: pavese@iummi4.terra.unimi.it*

(*Received 1 September 1995; accepted 20 December 1995*)

Abstract

Theoretical structure factors F_q of rhombohedral magnesite ($MgCO_3$) have been computed by quantum-mechanical periodic Hartree–Fock methods and compared with observed $|F_o|$ (literature data) and conventional F_c (independent-spherical-atom model) values. The corresponding R_{oq}, R_{oc} and R_{qc} agreement factors (overall values 2.03, 2.11 and 1.80%, respectively) are analysed *versus* $\sin(\theta)/\lambda$, showing the effects of chemical bonding and of experimental errors. Difference electron density maps $\Delta\rho_{oq}$, $\Delta\rho_{oc}$ and $\Delta\rho_{qc}$ have been calculated for the CO_3 and the C—O—Mg planes. Features of the C—O covalent bonding and oxygen lone pair are compared and discussed.

1. Introduction

Magnesite ($MgCO_3$) is an end-member mineral belonging to the class of rhombohedral carbonates; it is isomorphous to calcite (space group $R\bar{3}c$) but with a smaller cell. It usually occurs in nature as an alteration product of Mg-rich igneous and metamorphic rocks when CO_2 is available. Magnesium carbonate is a relevant technological material employed for the preparation, after heating and sintering, of magnesium oxide, a fundamental refractory material.

A number of authors dealt with structural and electron-density investigations on rhombohedral carbonates. The interest was principally focused on: (i) a debated order–disorder transition owing to a rotation of the CO_3 carbonate group upon heating (see, for instance, Markgraf & Reeder, 1985; Fiquet, Guyot & Itié, 1994); (ii) a possible pyramidal distortion of the CO_3 group, deviating from the planarity required by symmetry (see Effenberger, Kirfel & Will, 1983; Zemann, 1981); (iii) the nature of the cation–oxygen interaction (see Göttlicher & Vegas, 1988; Maslen, Streltsov & Streltsova, 1993*a*,*c*).

Electron-density analysis has been recently employed to investigate such aspects in magnesite. Göttlicher & Vegas (1988), hereafter GV, performed an accurate study about absolute and deformation-electron-density maps of magnesite, on ($xy1/4$) and ($x0z$) sections. Subsequently, Maslen, Streltsov & Streltsova (1993*a*, 1993*c*, indicated as MSS hereafter), carried out deformation-density analyses of magnesite and calcite, respectively, claiming the necessity to utilize an extinction-correction treatment that is independent of the structure refinement, in order not to bias the scale factor and the thermal parameters (Maslen & Spadaccini, 1993).

The determination of electron density by X-ray diffraction data is a quite delicate task, involving experimental and theoretical difficulties. Careful intensity-profile analyses of measured reflections are required in order to avoid scan-truncation losses, which are sufficient to affect the displacement parameters dramatically and produce unphysical effects on the evaluated electron density (Destro & Marsh, 1987; Denne, 1977). Moreover, scale-factor treatment, thermal diffuse scattering, absorption and extinction corrections may significantly bias the results, in case they are not fairly accounted for (Blessing, 1987). Finally, further uncertainties arise because the experimental electron density may be determined by a classical approach (for instance GV) *via* standard spherical-atom refinements and subsequent Fourier difference syntheses or by a generalized structure-factor formalism (Stewart, 1976), refining directly the population coefficients and radial coefficients of the multipolar expansion.

Discrepancies are revealed in a number of works found in the literature. In a recent paper on the corundum (Al_2O_3) deformation electron density, determined by synchrotron-radiation diffraction, Maslen, Streltsov & Streltsova (1993*b*) pointed out that "there are equally large discrepancies between the authors' interpretations of their maps. This motivated" them "to carry out further independent studies, aimed at identifying the source of the discrepancies between the published analyses". Their study gave results that show that a residual electron density between a pair of Al atoms exists, implying, consequently, an unlikely Al—Al bond. Kirfel & Eichhorn (1990) and Brown & Spackman (1993) performed electron-density analyses of corundum as well, based on multipolar expansion; no similar effect was observed. Moreover, slight discrepancies on difference-electron-density peak values are also present in the studies concerning magnesite by GV and MSS, although they might be attributed to statistical uncertainties.

Owing to the complexity of experimental electron-density determination, the capability to compute it on the basis of a full theoretical approach should play a fundamental role in assessing and interpreting experimental results, allowing one to detect possible spurious effects as a consequence of the difficulties stated above. Studies of this kind have been performed, for instance, on Be and CaF_2 (Dovesi, Pisani, Ricca & Roetti, 1982; Lichanot, Rerat & Catti, 1995). An analysis of earlier results on C (diamond), Si, BaF_2 and MgO is given by Dawson (1969).

Recently, Catti, Pavese, Dovesi & Saunders (1993) performed a LCAO quantum-mechanical study of magnesite, based on the periodic Hartree–Fock approximation, which dealt with the simulation of structural, elastic and electronic properties; the electron density was evaluated by a density matrix formalism (Pisani, Dovesi, & Roetti, 1988). The results of this theoretical work, and the recent determinations of the magnesite electron density by X-ray diffraction experiments from GV and MSS, suggested a study to assess and compare observed and theoretical data. The Fourier expansion coefficients ($|F_q|$) of the theoretical quantum electron density are analysed *versus* experimental ($|F_o|$) and independent-atom model (IAM) ($|F_c|$) amplitudes; moreover, deformation-electron-density maps, computed through Fourier summations of the terms $F_o - F_q$ ($\Delta\rho_{oq}$), $F_o - F_c$ ($\Delta\rho_{oc}$) and $F_q - F_c$ ($\Delta\rho_{qc}$) are evaluated and discussed.

2. Computational method

The theoretical structure factors and electron density were computed by the *CRYSTAL* program (Dovesi, Pisani, Roetti, Causà & Saunders, 1989), which performs periodic self-consistent *ab initio* LCAO Hartree–Fock calculations, yielding the crystal energy and a number of properties of the solid (*i.e.* electron density, density of energy states, band structure). Contracted Gaussian-type functions were used to describe the atomic orbitals $\chi_i(\mathbf{r})$, which were employed as the basis set for the calculation of the crystal Bloch functions (details in Catti, Pavese, Dovesi & Saunders, 1993). Atomic orbitals, which consist of linear combinations of radial Gaussian functions multiplied by real solid harmonic functions, may be collected into shells characterized by the same radial part; five shells were employed for Mg and O, and four for C. The corresponding basis sets contain 18, 18 and 14 atomic orbitals, and are denoted as 8-511G*, 8-411G* and 6-21G* (Hehre, Radom, Schleyer & Pople, 1986) for Mg, O and C, respectively. Thus, their quality is of TZP (triple-zeta + polarization) type for Mg and O, and DZP (double-zeta + polarization) for C. The exponential coefficients of the Gaussian functions belonging to the outermost *sp* shells were optimized numerically by minimizing the total crystal energy.

The electron density is calculated by the expression

$$\rho_q(\mathbf{r}) = \sum_{ij} \sum_{\mathbf{l}} P_{ij}(\mathbf{l}) \chi_i(\mathbf{r}) \chi_j(\mathbf{r} - \mathbf{l}), \qquad (1)$$

where $\mathbf{r}$ is the position vector of the electron in the unit cell, $\mathbf{l}$ is a direct-lattice vector and $P_{ij}(\mathbf{l})$ is a component of the direct-space density matrix corresponding to the ground-state wave-function solution of the Hartree–Fock equations. By Fourier transforming the above formula, the static ($T = 0$ K) structure factors are obtained as a function of the reciprocal-lattice vector $\mathbf{h}$:

$$F_q(\mathbf{h}) = \sum_{ij} \sum_{\mathbf{l}} P_{ij}(\mathbf{l}) \int \chi_i(\mathbf{r}) \chi_j^*(\mathbf{r} - \mathbf{l}) \exp(2\pi i \mathbf{h} \cdot \mathbf{r})\, d\mathbf{r}. \qquad (2)$$

However, for comparison with the experimental data, the temperature effect has to be accounted for in the theoretical results. Some sophisticated methods have been recently developed for this purpose (Lichanot, Rerat & Catti, 1995), but in this case a simpler, yet quite satisfactory, approach is adopted. Every static theoretical structure factor F_q is multiplied by the ratio of the corresponding F_c (room-temperature IAM refinement) to the value evaluated with vanishing thermal parameters. Furthermore, the experimental electron density is affected by truncation errors of the Fourier series; these are small because data up to $\sin(\theta)/\lambda \simeq 1$ Å^{-1} have been used by GV and MSS, but not vanishing. For these two reasons, the theoretical ρ_q obtained by (1) is not suitable for comparison with the experimental densities; instead, ρ_q has been calculated by Fourier transformation of (2), limited by the same $[\sin(\theta)/\lambda]_{max}$ threshold used by GV and MSS, and using F_q values corrected for temperature effects* as described above.

The experimental amplitudes of $MgCO_3$ by GV and MSS were obtained from the supplementary publications deposited by the authors with the IUCr. These $|F_o|$ data are already corrected for absorption, extinction and thermal diffuse scattering, and they are reported on an absolute scale. Conventional structural refinements were carried out on both observed data sets in a slightly different way with respect to the original ones, in order to avoid any possible bias in F_c values, owing to an inappropriate determination of thermal parameters. Therefore, high-angle experimental reflections [$\sin(\theta)/\lambda \geq 0.6$ Å^{-1}] only were employed to refine the coordinates and displacement factors, with scale fixed at 1.0. Scattering factors from *International Tables for Crystallography* (1992) were employed; the weights are unitary and $1/\sigma^2(|F_o|)$ for GV and MSS data, respectively, according to the original treatments. Anomalous dispersion was included in F_c values, though

* A list of theoretical structure factors of $MgCO_3$, corrected for room-temperature and anomalous-scattering effects, has been deposited with the IUCr (Reference: SH0075). Copies may be obtained through The Managing Editor, International Union of Crystallography, 5 Abbey Square, Chester CH1 2HU, England.

the effect for Mg, O and C atoms with Mo $K\alpha$ radiation is very small and even high-angle reflections are affected in a minor way only (the largest phase is 8°). For the sake of comparison, every theoretical $|F_q|$ was rescaled by the ratio of the corresponding $|F_c|$ moduli evaluated with and without anomalous dispersion. The signs of all F_q match exactly the corresponding ones of F_c uncorrected for anomalous dispersion. The refined structural parameters confirm those obtained by GV and MSS, with differences oscillating within 3σ and, therefore, they are not reported here. Quantum-mechanical calculations were performed employing the refined structures.

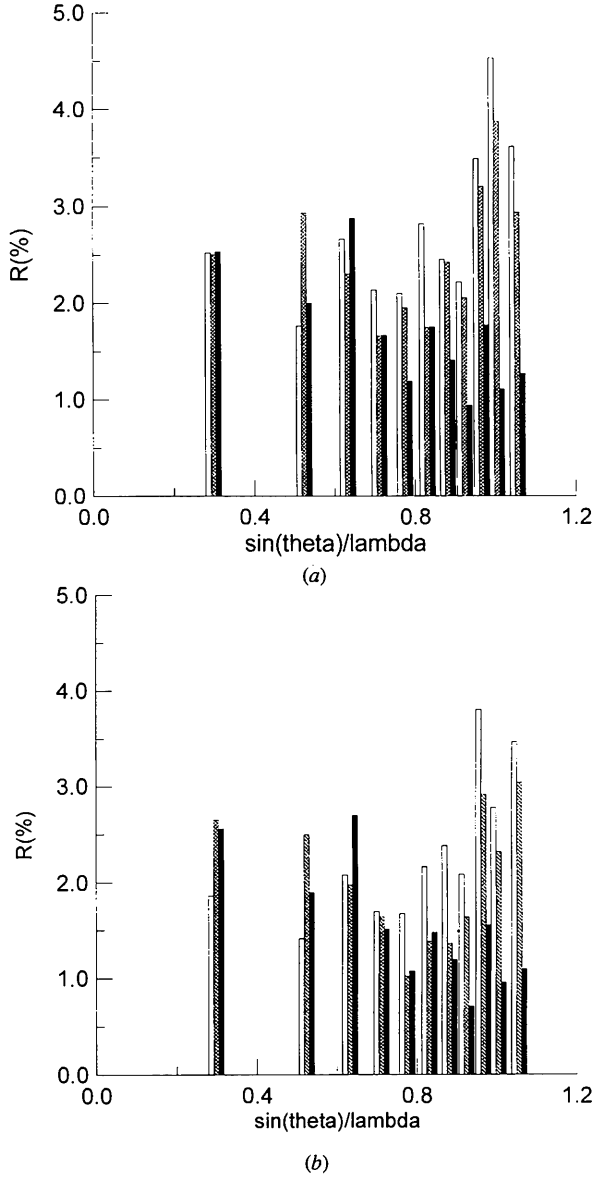

Fig. 1. (*a*) Histograms of the figures of merit $R_{ab} = \sum_{\mathbf{h}} ||F_a(\mathbf{h})| - |F_b(\mathbf{h})|| / \sum_{\mathbf{h}} |F_a(\mathbf{h})|$ *versus* $\sin(\theta)/\lambda$ for 300 reflections of $MgCO_3$; each channel contains about 30 reflections. F_o and F_c are from Göttlicher & Vegas (1988) data, while F_q are theoretical structure factors. The white, grey and black columns correspond to R_{oq}, R_{oc} and R_{qc}, respectively. (*b*) As (*a*) but referred to the data of Maslen, Streltsov & Streltsova (1993*c*) (300 reflections).

3. Results and discussion

3.1. *Structure factors*

The structure factors F_q, F_c and F_o have been mutually compared, employing both GV and MSS experimental data sets. Reflections have been distributed into $\sin(\theta)/\lambda$ shells, each consisting of about 30 members and the following comparisons have been performed: F_o *versus* F_c, F_o *versus* F_q and F_q *versus* F_c. The corresponding figures of merit $R_{ab} = \sum_{\mathbf{h}} ||F_a(\mathbf{h})| - |F_b(\mathbf{h})|| / \sum_{\mathbf{h}} |F_a(\mathbf{h})|$ (hereafter R_{oc}, R_{oq} and R_{qc}, respectively) have been evaluated and reported *versus* $\sin(\theta)/\lambda$ in the histograms of Figs. 1(*a*) and (*b*). F_q and F_c structure factors were calculated for both structures refined from the GV (300 reflections) and MSS (330 reflections) observed intensities and compared with the respective experimental data. Comparisons involving MSS data have been carried out by extracting the subset of reflections corresponding to those of GV.

As expected, R_{qc} turns out to decrease with increasing $\sin(\theta)/\lambda$, since the structure factors computed by the spherical independent-atom model (F_c) better match high-angle theoretical quantum reflections, less affected by chemical bonding effects that cause deviations from the independent-atom model. The oscillations observed in the decreasing trend of R_{qc} are probably related to atomic basis-set differences between the present quantum-mechanical scheme and that used to derive standard atomic scattering factors. An opposite trend is shown by R_{oq}: at low $\sin(\theta)/\lambda$, the agreement is very good (*cf.* particularly Fig. 1*b*) because the theoretical F_q values account well for chemical bonding, while at high angles the F_o's are largely influenced by experimental errors, typical of weak reflections, so that R_{oq} worsens. The conventional crystallographic agreement factor, R_{oc}, has an intermediate behaviour, resembling R_{qc} (decreasing trend) and R_{oq} (increasing trend) at small and large $\sin(\theta)/\lambda$, respectively. This is due to F_o behaving like F_q at low angles, where bonding effects dominate, and to F_c behaving like F_q at high angles, where experimental uncertainties dominate (provided that systematic errors have been properly corrected for).

By comparing the results of R_{qc}, R_{oq} and R_{oc} *vs* $\sin(\theta)/\lambda$ for the GV and MSS data sets, it appears that: (i) the R_{qc} values are nearly the same in both cases; (ii) the behaviour of R_{oq} and R_{oc} is more regular [R_{oq} increasing, R_{oc} at first decreasing and then increasing with $\sin(\theta)/\lambda$] for MSS than for GV data. In particular, at low angles, $R_{oq} \leq R_{oc}$ in the MSS case, as expected on general grounds, while $R_{oq} \simeq R_{oc}$ for GV results. Thus, a slightly better quality of MSS data with respect to GV data can be inferred. This is confirmed by

comparing the overall figures of merit R_{qc}, R_{oq} and R_{oc} calculated for all reflections: 0.0180, 0.0203, 0.0211 (MSS) and 0.0192, 0.0251, 0.0246 (GV), respectively.

3.2. *Difference-electron-density maps*

Since we achieved similar results on difference-electron-density maps employing GV and MSS experimental data sets, hereafter in the discussion the latter ones only are referred to. An estimated uncertainty of $0.03\,e\,Å^{-3}$ is reported for the experimental electron density in MSS's paper.

The $\Delta\rho_{qc}$ and $\Delta\rho_{oc}$ difference maps, for the section ($xy1/4$), which contains the CO_3 molecular group, are shown in Figs. 2(*a*) and (*b*), respectively. Quite similar bonding charges ($0.5\,e\,Å^{-3}$) located midway between C and O appear in both maps, so that a consistent picture of the C—O covalent bond arises from Hartree–Fock theory and MSS (or GV) experimental data. Negative peaks in the neighbourhood of nuclear positions indicate a spreading in the space of valence electrons when passing from isolated to bonded atoms in the crystal. This effect is similar in the two maps for carbon, but different for oxygen: the well is $-0.2\,e\,Å^{-3}$ deep and located at the O nucleus site for $\Delta\rho_{oc}$, while it is deeper and shifted towards carbon for $\Delta\rho_{qc}$. In a related way, the positive peaks of the O lone-pair region are $0.2\,e\,Å^{-3}$ higher and located closer to the O atom in the $\Delta\rho_{qc}$ with respect to the $\Delta\rho_{oc}$ case. Thus, quantum-mechanical results would indicate a stronger (but more contracted in space towards carbon) polarization of the

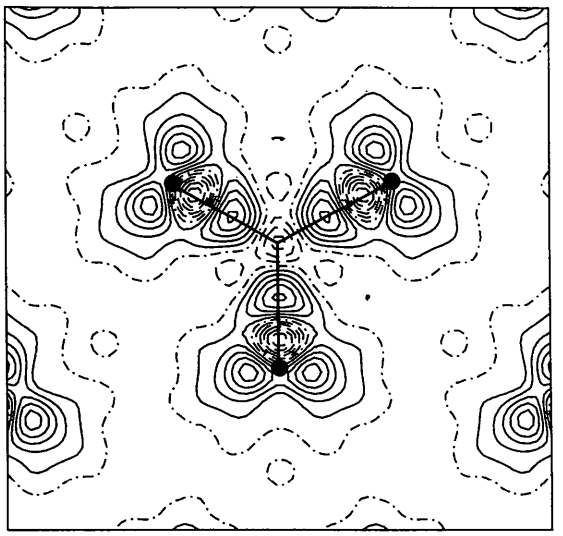

(*a*)

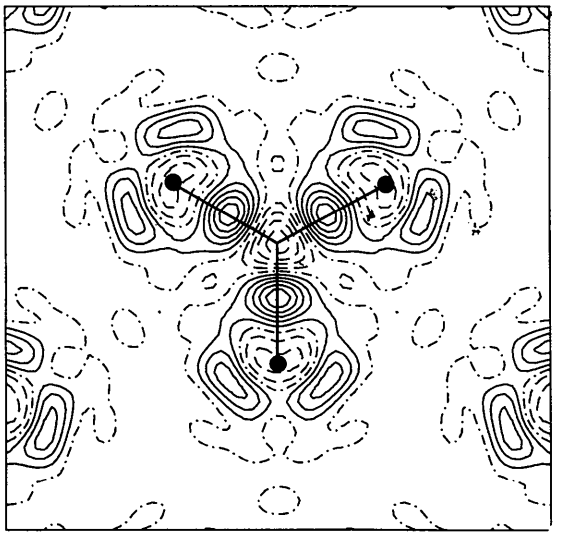

(*b*)

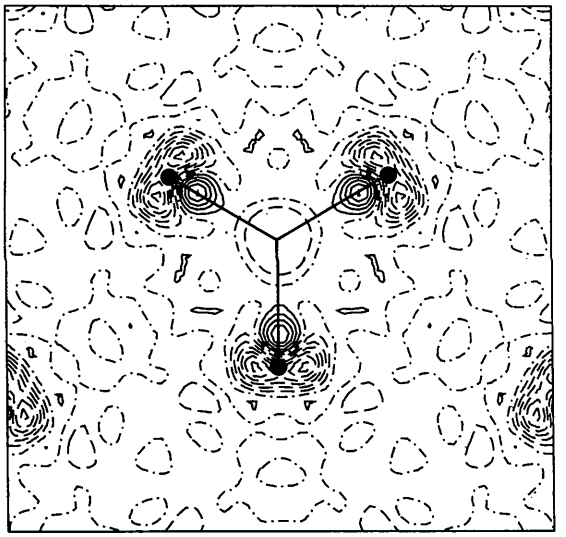

(*c*)

Fig. 2. (*a*) Difference-electron-density map ($\Delta\rho_{qc}$) on the section ($xy1/4$), containing the carbonate group, obtained by Fourier transform of $F_q - F_c$. C—O bonds are denoted by straight lines. The F_c values come from MSS data. Full, dashed and dot-dashed contour lines refer to positive, negative and zero values, respectively. The interval between isolines is $0.1\,e\,Å^{-3}$. (*b*) Difference-electron-density map ($\Delta\rho_{oc}$) on the section ($xy1/4$). F_o values from MSS data. (*c*) Difference-electron-density map ($\Delta\rho_{oq}$) on the section ($xy1/4$).

O electron cloud through chemical bonding, with respect to that observed for experimental data.

These results are confirmed by looking at the $\Delta\rho_{oq}$ map in the same section (Fig. 2*c*). No difference density appears in the middle of the C—O covalent bond. The positive peaks close to O atoms on the C side and the negative ones in lone-pair positions indicate a larger transfer of oxygen electron density from the inner to the outer region of the CO_3 group in the case of theoretical with respect to the experimental results. At the same time, in the former case, O lone pairs are less diffuse in space than in the latter. Such discrepancies between Hartree–Fock and experimental electron densities in the neighbourhood of O atoms are, however, comparatively modest, and may be related either to neglect of electron correlation in theoretical results or to deficiencies in corrections for thermal motion and other systematic effects affecting experimental data.

The Mg atom placed at the origin of the reference axes and the nearest C and O atoms belonging to the same CO_3 group define the section ($xyy/4$); the corresponding difference electron densities $\Delta\rho_{qc}$, $\Delta\rho_{oc}$ and $\Delta\rho_{oq}$ are presented in Figs. 3(*a*), (*b*) and (*c*), respectively. As above, the main features of the $\Delta\rho_{qc}$ and $\Delta\rho_{oc}$ maps agree, although the same slight differences concerning the charge distribution of the O atom and its lone pairs appear here, too. In particular, the maxima of the lone pairs look more diffuse and slightly displaced towards Mg in the the case of $\Delta\rho_{oc}$. Their positions have been estimated to lie about 0.1 Å away from the plane of the section ($xyy/4$), by calculating $\Delta\rho_{qc}$ on a number of sections parallel to ($xyy/4$) and interpolating the obtained

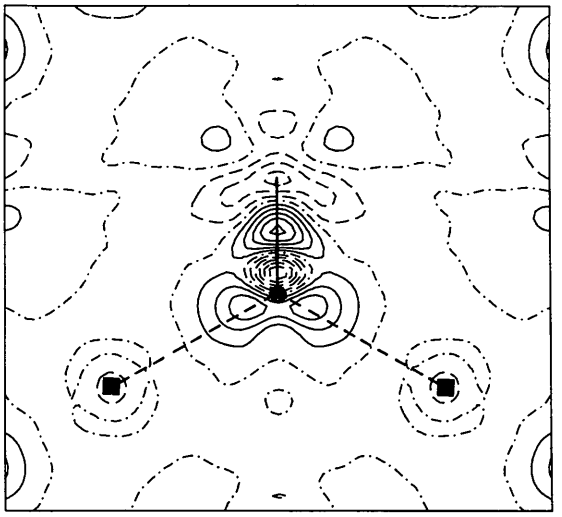

(*a*)

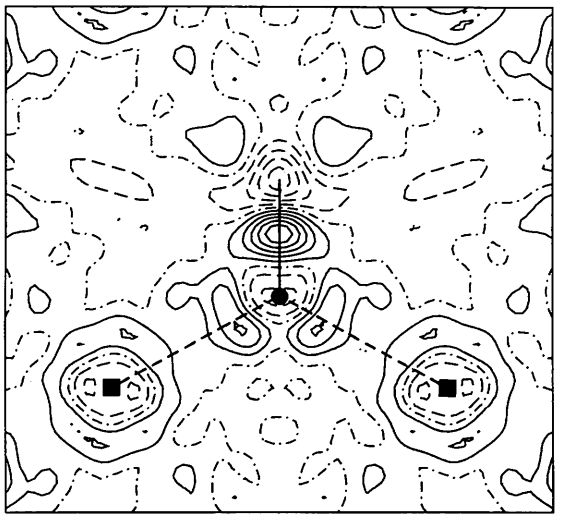

(*b*)

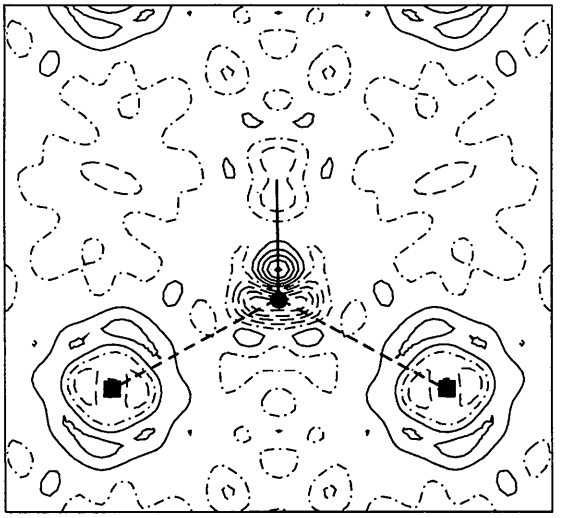

(*c*)

Fig. 3. (*a*) Difference-electron-density map ($\Delta\rho_{qc}$) on the section ($xyy/4$). F_c values are based on MSS data. Full and dashed straight lines denote the C—O and Mg—O bonds, respectively; O and Mg are represented by circles and squares. Other symbols and interval between isolines as in Fig. 2(*a*). (*b*) Difference-electron-density map ($\Delta\rho_{oc}$) on the section ($xyy/4$). F_o values from MSS data. (*c*) Difference-electron-density map ($\Delta\rho_{oq}$) on the section ($xyy/4$).

results. A slight positive residual density is observed on Mg atoms in the $\Delta\rho_{oc}$ map.

4. Conclusions

The periodic Hartree–Fock quantum-mechanical approach has proved quite powerful in calculating reliable *ab initio* structure factors and electron density of a comparatively complex crystal like $MgCO_3$. All relevant features of chemical bonding appear correctly in theoretical density maps, including the C—O covalent bond and oxygen lone-pair densities and in good overall agreement with experimental diffraction results. Slight differences are observed in details of the electron-charge distribution close to O atoms. The theoretical structure factors agree very well with the observed and the calculated (independent-spherical-atom model) ones at low and high diffraction angles, respectively. This indicates that the use of first-principles *ab initio* structure factors may be an attractive way to check for suspected experimental errors or insufficient correction of physical effects in X-ray observed data sets.

References

Blessing, R. H. (1987). *Crystallogr. Rev.* **1**, 3–58.

Brown, A. & Spackman, M. A. (1993). *Acta Cryst.* A**49**, 513–527.

Catti, M., Pavese, A., Dovesi, R. & Saunders, V. (1993). *Phys. Rev. B*, **47**, 9189–9198.

Dawson, B. (1969). *Acta Cryst.* A**25**, 12–28.

Denne, W. A. (1977). *Acta Cryst.* A**33**, 438–440.

Destro, R. & Marsh, R. E. (1987). *Acta Cryst.* A**43**, 711–718.

Dovesi, R., Pisani, C., Ricca, F. & Roetti, C. (1982). *Phys. Rev. B*, **25**, 3731–3739.

Dovesi, R., Pisani, C., Roetti, C., Causà, M. & Saunders, V. R. (1989). *CRYSTAL*88. Program No. 577, Quantum Chemistry Program Exchange, Indiana University, Bloomington, IN, USA.

Effenberger, H., Kirfel, A. & Will, G. (1983). *Tschermaks Mineral. Petrogr. Mitt.* **31**, 233–243.

Fiquet, G., Guyot, F. & Itié, J. (1994). *Am. Mineral.* **79** 15–23.

Göttlicher, S. & Vegas, A. (1988). *Acta Cryst.* B**44**, 362–367.

Hehre, W. H., Radom, L., Schleyer, P. R. & Pople, J. A. (1986). *Ab initio Molecular Orbital Theory*. New York: Wiley.

International Tables for Crystallography. (1992). Vol. C. Dordrecht/Boston/London: Kluwer.

Kirfel, A. & Eichhorn, K. (1990). *Acta Cryst.* A**46**, 271–284.

Lichanot, A., Rerat, M. & Catti, M. (1995). *Acta Cryst.* A**51**, 323–328.

Markgraf, S. A. & Reeder, R. J. (1985). *Am. Mineral.* **70**, 590–600.

Maslen, E. N. & Spadaccini, N. (1993). *Acta Cryst.* A**49**, 661–667.

Maslen, E. N., Streltsov, V. A. & Streltsova, N. R. (1993*a*). *Acta Cryst.* B**49**, 636–641.

Maslen, E. N., Streltsov, V. A. & Streltsova, N. R. (1993*b*). *Acta Cryst.* B**49**, 973–980.

Maslen, E. N., Streltsov, V. A. & Streltsova, N. R. (1993*c*). *Acta Cryst.* B**49**, 980–984.

Pisani, C., Dovesi, R. & Roetti, C. (1988). *Hartree–Fock Ab Initio Treatement of Crystalline Solids. Lecture Notes in Chemistry*, Vol. 48. Berlin: Springer Verlag.

Stewart, R. (1976). *Acta Cryst.* A**32**, 565–574.

Zemann, J. (1981). *Fortschr. Mineral.* **59**, 95–116.